Supplementary Materials

Femtosecond Laser Ablation of a Bulk Graphite Target in Water for Polyyne and Nanomaterial Synthesis

Nikolaos G. Semaltianos [1,*], Ona Balachninaitė [2], Remigijus Juškėnas [3], Audrius Drabavicius [3], Gediminas Niaura [4] and Euan Hendry [5]

[1] Department of Physics, Aristotle University of Thessaloniki, 54124 Thessaloniki, Greece
[2] Laser Research Center, Vilnius University, Saulėtekio av. 10, 10223 Vilnius, Lithuania
[3] Department of Characterization of Materials Structure, Center for Physical Sciences and Technology—FTMC, Saulėtekio av. 3, 10257 Vilnius, Lithuania
[4] Department of Organic Chemistry, Center for Physical Sciences and Technology (FTMC), Saulėtekio av. 3, 10257 Vilnius, Lithuania
[5] Department of Physics, University of Exeter, Exeter EX4 4QL, UK
* Correspondence: nsemaltianos@yahoo.com

For comparison with the LIBS spectra measured in DI water spectra were also measured upon target ablation in ambient air (Figure S1). With a pulse energy of 50 μJ relatively strong C_2 Swan bands corresponding to the Δv=+1, 0, and -1 transitions ($d\ ^3\Pi_g$—$a\ ^3\Pi_u$) were detected at: 468.53 (4,3), 469.70 (3,2), 471.51 (2,1), 473.68 nm (1,0) (Figure S2a); 516.47 nm (0,0) (Figure S2b); and 558.54 (1,2) and 563.52 nm (0,1) (Figure S2c), respectively. In UV ns laser ablation (193 nm, excimer laser, 10 Hz) in vacuum no C_2 molecular bands were observed - only lines from C atomic and ionic species [35]. The bands are still present in the spectra even for the longest measured time delay of 300 ns. This relatively long persistence of the band emission is due to collisions of species in the plasma during expansion. At the present case of a fs laser ablation the formation of C_2 molecules most likely occurs by the interaction and dimerization of two C atoms that occurs before their ionization and conversion to ions [$2C \rightarrow C_2$] or with a lower probability by the dissociation of larger clusters (C_n) to C_2 dimers due to the resulting relatively high fluence used (melting and vaporization rather than sublimation) [36,37]. The vibrational/rotational temperatures of the C_2 molecules were determined by theoretical fitting to the Δv=-1 Swan band (high intensity peaks at 563.52 and 558.54 nm and lower intensity peaks in between those, corresponding to rotational transitions of the molecule) using the open source code BESP-NMT [38,39] (Figure S3) and the resulting temperature versus time delay is shown in Figure S4. A temperature from ~3300 to ~1800 K is determined for a time delay from ~140 to ~250 ns for 50 uJ pulse energy. Higher rotational temperatures in the range of 5100−4300 K for delays 500−2000 ns have been determined in the case of a ns laser ablation (20 ns/1064 nm) whereas the temperature cooling rate of the plume was higher during ablation of the target in water (from 5600 to 3500 K for 500 to 1200 ns) compared to air (from 5100 to 5300 K during the same time interval) attributed to the more effective cooling of the plume by the water [40]. Under ablation in vacuum (6 ns/1064 nm) the plasma temperature was found to increase from ~9800 to ~15000 K with the increase of the pressure from ~150 to ~1000 mbar attributed to the higher collisional interaction of the plasma particles (electrons, ions, and neutrals) due to the plume compression [41]. In the case of a fs ablation (40 fs/800 nm/10 Hz) in nitrogen gas atmosphere a C_2 vibrational temperature of ~12760 K was determined at ~1 Torr gas pressure decreasing to ~8100 K at ~10 Torr whereas at helium gas atmosphere lower temperatures of ~8700 and ~6960 K at the above pressures, respectively were determined [37]. A relatively low black-body plasma plume temperature of ~2900±200 K comparable to that determined in the present work was determined in the case of UV fs ablation (450 fs/248 nm) of graphite in vacuum (5×10^{-7} Torr) [42].

Other carbon-related lines that are detected in the spectra are a CI line at 833.65 mm ($2s^22p3s\ ^1P^o_1 \leftarrow 2s^22p3p\ ^1S_0$) (Figure S5a) and the CII line at 868.25 nm (Figure S5b) (the peaks due to NI on the left and right hand side of the 868.25 nm peak, at 868.04 and 868.39 nm, respectively are also distinguished). Observation of emission from neutral carbon atoms here contrary to the case of a fs or ps laser ablation (248 ns; 450 fs or

5 ps; fluences 2.1 or 3.6 J/cm^2, respectively) of graphite in vacuum where only carbon ionic lines are observed [42] may be due to the collisional neutralization of CII ions by electrons originating from air species.

Other lines that are distinguished in the spectra are: NI (744.32 nm), NI (746.96 nm), OI (777.41 nm), NI (818.79 nm), NI (821.71 nm), OI (844.73 nm), and NI (871.95 nm) (Figure S1).

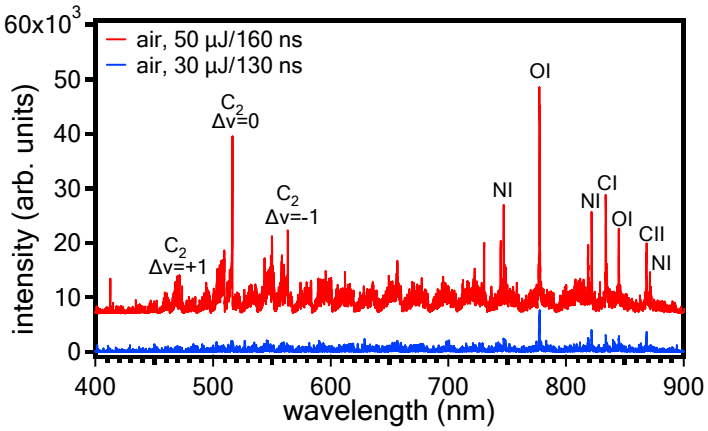

Figure S1. LIBS spectra measured upon ablation of the target in air at 50 µJ/6 kHz and 30 µJ/6 kHz.

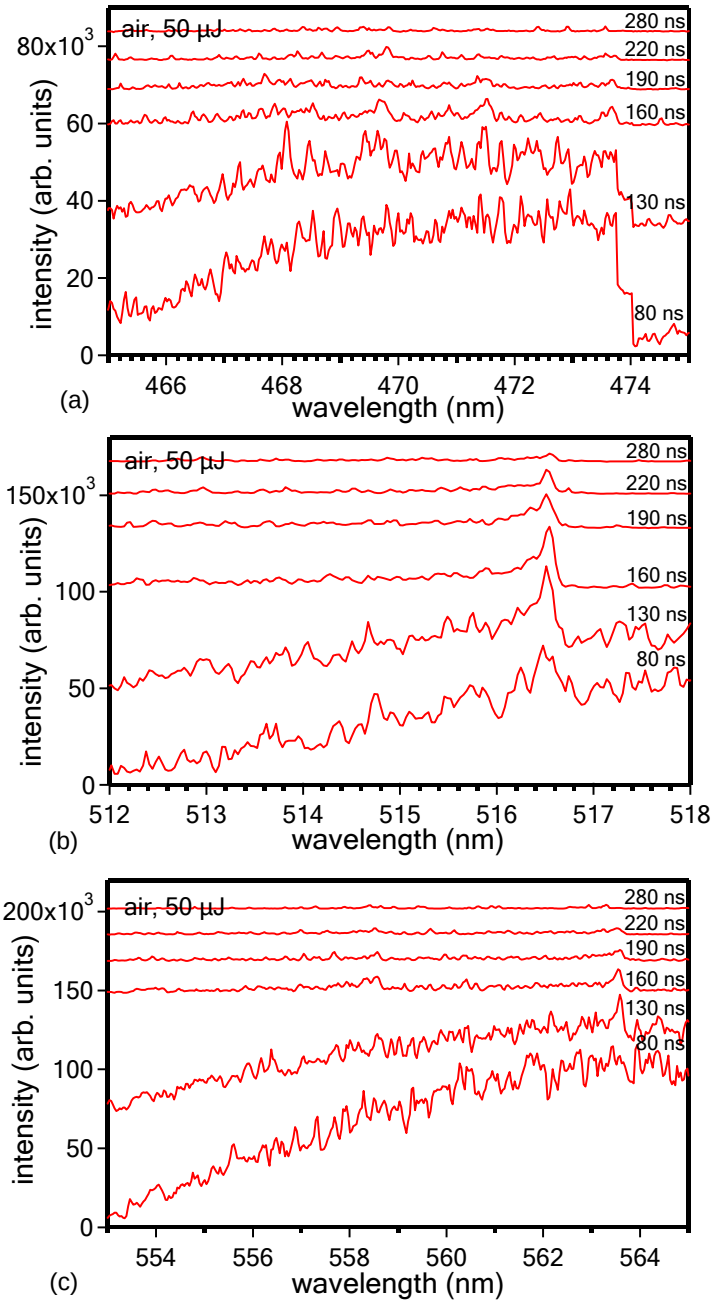

Figure S2. LIBS spectra measured upon ablation of the target in air at 50 µJ/6 kHz and for different time delays in the region of 465–475 (a), 512–518 (b), and 553–565 nm (c) where the C_2 Swan bands due to Δv=+1, 0, and -1 transitions appear, respectively.

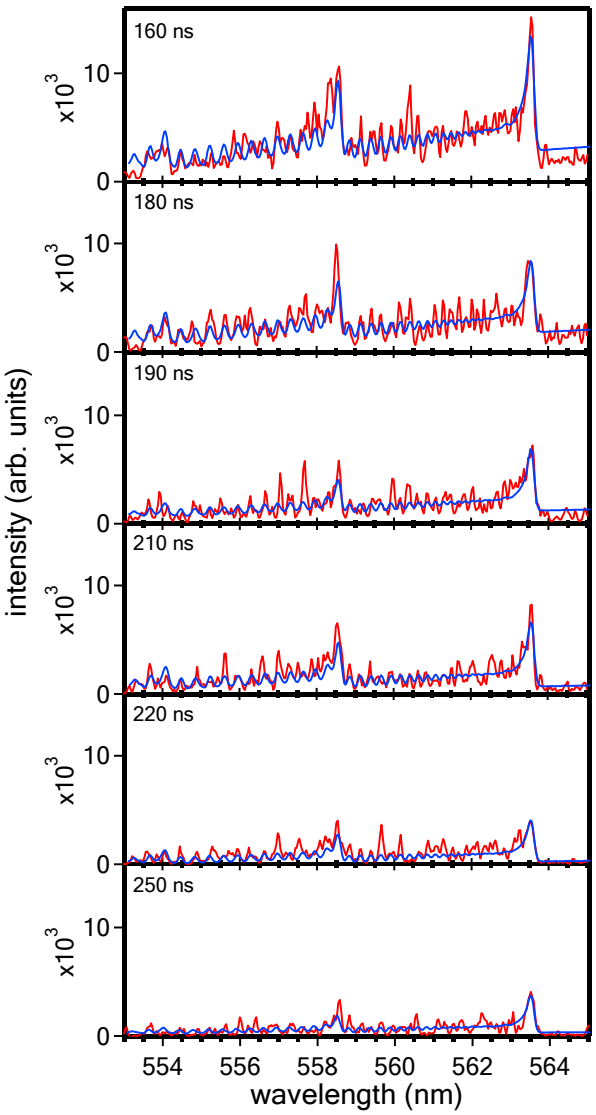

Figure S3. LIBS spectra measured for different time delays in the region of 553–565 nm where the C_2 Swan bands corresponding to Δv=-1 transitions appear. The blue lines correspond to theoretical fitting to the experimentally measured spectra (red lines).

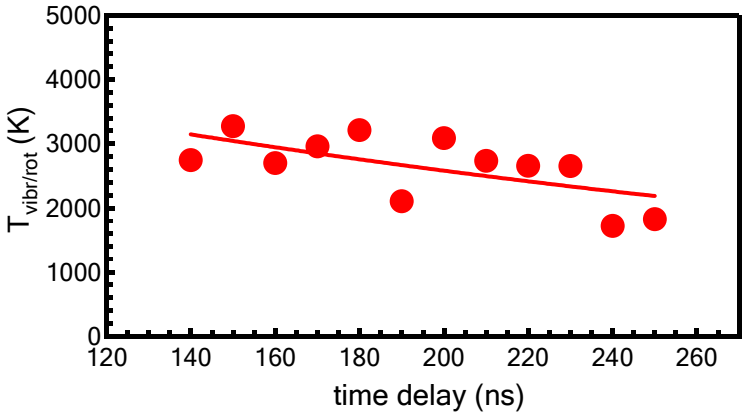

Figure S4. Vibrational/rotational temperature of the C_2 molecules versus the time delay as determined from the theoretical fitting of Figure S3.

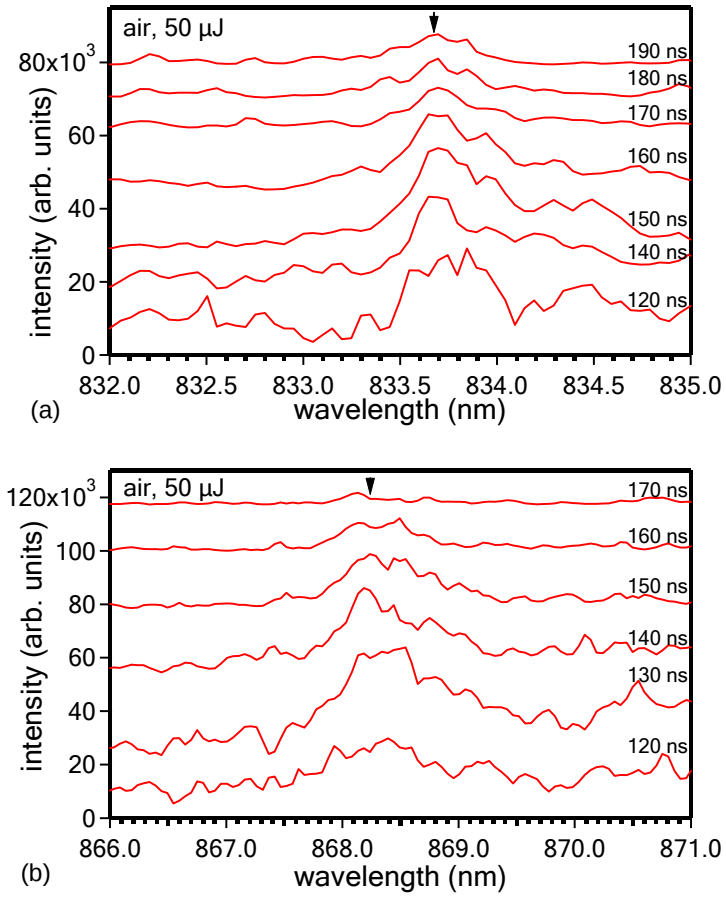

Figure S5. LIBS spectra measured with different time delays upon ablation (50 µJ/6 kHz) of the target in air, showing the CI line at 833.65 nm (a) and CII line at 868.25 nm (b).

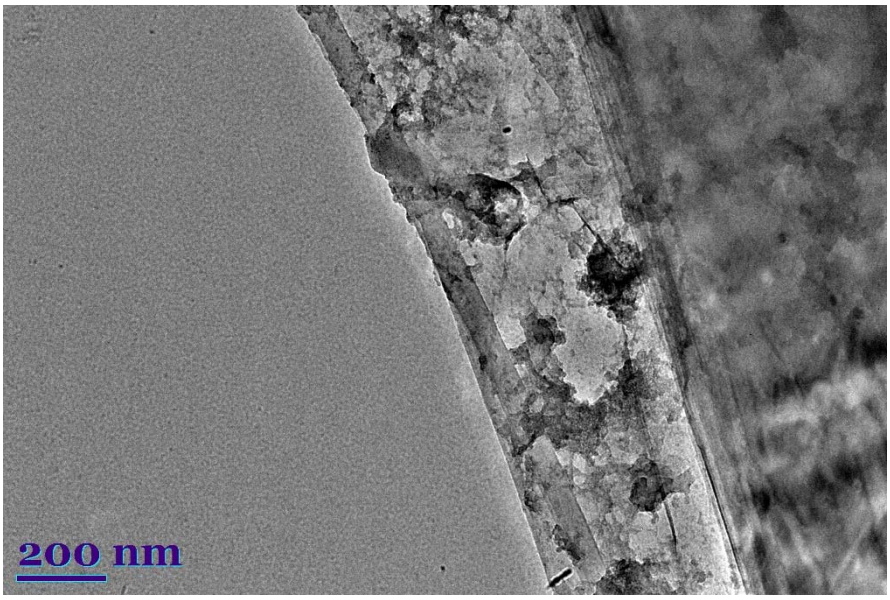

Figure S6. TEM image of the sheet-like structures in the ablation products (DI water, 80 μJ/6 kHz, 33 min). The large NPs are distinguished on the sheets and in the spaces between them.

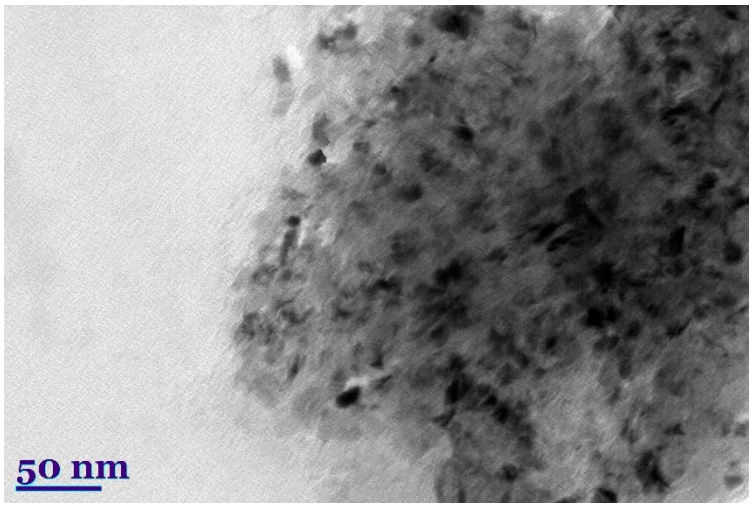

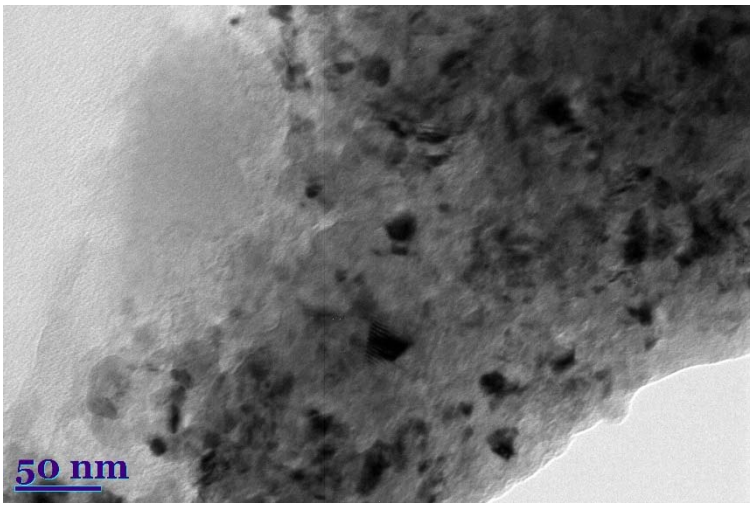

Figure S7. TEM images of the ablation products (DI water, 800 nm/110 μJ).

References

35. Claeyssens, F.; Lade, R. J.; Rosser, K. N.; Ashfold, M. N. R. Investigations of the plume accompanying pulsed ultraviolet laser ablation of graphite in vacuum. *J. Appl. Phys.* **2001**, *89*, 697−709.
36. Wakisaka, A.; Gaumet, J. J.; Shimizu, Y.; Tamori, Y.; Sato, H.; Tokumaru, K. Growth of Carbon Clusters. *J. Chem. Soc. Farad. Trans.* **1993**, *89(7)*, 1001−1005.
37. Al-Shboul, K. F.; Harilal, S. S.; Hassanein, A. Emission features of femtosecond laser ablated carbon plasma in ambient helium. *J. Appl. Phys.* **2013**, *113*, 163305−163314.
38. Parigger, C. G.; Woods, A. C.; Surmick, D. M.; Gautam, G.; Witte, M. J.; Hornkohl, J. O. Computation of diatomic molecular spectra for selected transitions of aluminium monoxide, cyanide, diatomic carbon, and titanium monoxide. *Spectr. Chim. Act. B* **2015**, *107*, 132−138.
39. Parigger, C. G. Diatomic Line Strengths for Fitting Selected Molecular Transitions of AlO, C_2, CN, OH, N_2^+, NO, and TiO, Spectra. *Foundations* **2023**, *3*, 1−15.
40. Saito, K.; Sakka, T.; Ogata, Y. H. Rotational spectra and temperature evaluation of C_2 molecules produced by pulsed laser irradiation to a graphite-water interface. *J. Appl. Phys.* **2003**, *94*, 5530−5536.
41. Chaudhary, K.; Rosalan, S.; Aziz, M. S.; Bohadoran, M.; Ali, J.; Yupapin, P. P.; Bidin, N.; Saktioto, Laser-Induced Graphite Plasma Kinetic Spectroscopy under Different Ambient Pressures. *Chin. Phys. Lett.* **2015**, *32*, 043201−043206.
42. Claeyssens, F.; Ashfold, M. N. R.; Sofoulakis, E.; Ristoscu, C. G.; Anglos, D.; Fotakis, C. Plume emissions accompanying 248 nm laser ablation of graphite in vacuum: Effects of pulse duration. *J. Appl. Phys.* **2002**, *91*, 6162−6172.